

Ubiquitous Symmetry at Critical Points Across Diverse Optimization Landscapes

Irmi Schneider
 The Hebrew University of Jerusalem
 Department of Computer Science
 irmi.schneider@mail.huji.ac.il

Abstract

Symmetry plays a crucial role in understanding the properties of mathematical structures and optimization problems. Recent work has explored this phenomenon in the context of neural networks, where the loss function is invariant under column and row permutations of the network weights. It has been observed that local minima exhibit significant symmetry with respect to the network weights (invariance to row and column permutations). And moreover no critical point was found that lacked symmetry. We extend this line of inquiry by investigating symmetry phenomena in real-valued loss functions defined on a broader class of spaces. We will introduce four more cases: the projective case over a finite field, the octahedral graph case, the perfect matching case, and the particle attraction case. We show that as in the neural network case, all the critical points observed have non-trivial symmetry. Finally we introduce a new measure of symmetry in the system and show that it reveals additional symmetry structures not captured by the previous measure.

Contents

1	Introduction	2
1.1	Main results of this paper	4
2	Optimization on the Projective Space	5
2.1	Introduction	5
2.2	Loss Definition	6
2.3	Results	6
2.4	Results For Reformulated Loss	7
3	Optimization on the Octahedral Graph	7
3.1	Loss Definition	7
3.2	Results	8
4	Optimization on the Perfect Matching Graph	9
4.1	Loss Definition	9
4.2	Results	9
5	Particle Attraction Case	10
5.1	Loss Definition	10
5.2	Results	10
5.3	Robustness Under Varying Kernel Functions and High-Degree Polynomials	11
5.4	Narrow Attraction Basins of Non-Symmetric Minima (if they indeed exist)	12

6	New Measure of Symmetry - Edge Isotropy Group I_E	12
6.1	Introduction	12
6.2	Edge Isotropy Group Definition I_E	12
6.3	I_E Isotropy Group for $n = 4, n = 7$ ($\kappa(x, y) = \ x - y\ ^{12} - \ x - y\ ^8$ kernel)	12
6.4	Experiments for $n = 4$ and $n = 7$ with $\kappa = \ \mathbf{a} - \mathbf{b}\ ^2 + \frac{1}{\ \mathbf{a} - \mathbf{b}\ ^2}$ Kernel	13
6.5	Summary of the Edge Isotropy Group I_E	14
7	Summary	14
	Appendix	16
A	Detailed Experimental Data for the Projective Plane over the Field \mathbb{F}_2	16
B	Plots for particle attraction case	18
B.1	Plots for 4 particles Experiments (kernel $d^{12} - d^8$)	18
B.2	Plots for 7 particles Experiments (kernel $d^{12} - d^8$)	20
B.3	Plots for 4 particles Experiments (kernel $d^2 + \frac{1}{d^2}$)	25
B.4	Plots for 7 particles Experiments (kernel $d^2 + \frac{1}{d^2}$)	26
C	Symmetry in Loss Landscapes: Particle Attraction vs. Random Polynomial Experiments	28
D	Symmetric Particle Attraction Experiment	28
E	Particle Attraction Case For Random 4 degree kernel	29

1 Introduction

The optimization of neural networks is a central challenge in machine learning. Recent research has emphasized the importance of *symmetry* in understanding the optimization landscape, particularly for shallow ReLU networks. In this context, [Arjevani and Field \[2019\]](#) consider the population loss minimization problem

$$\mathcal{L}(W) := \frac{1}{2} \mathbb{E}_{x \sim \mathcal{N}(0, I_d)} \left[\left(\mathbf{1}_d^\top \phi(Wx) - \mathbf{1}_d^\top \phi(Vx) \right)^2 \right], \quad (1)$$

where:

- $W \in M(d, d)$ is the weight matrix,
- $V \in M(d, d)$ is the target weight matrix, fixed as $V = I_d$,
- $\phi: \mathbb{R} \rightarrow \mathbb{R}$ is the ReLU activation function, defined by $\phi(z) := \max\{0, z\}$,
- $\mathbf{1}_d \in \mathbb{R}^d$ is the vector of all ones.

Similarly, [Arjevani et al. \[2021\]](#) investigate the symmetry of local minima in symmetric tensor decomposition. They study the optimization problem

$$\min_{W \in M(d, d)} L_\star(W) := \left\| \sum_{i=1}^d w_i^{\otimes n} - T \right\|_\star^2, \quad (2)$$

where:

- w_i denotes the i th row of W ,
- $\otimes n$ represents the n -fold tensor product,

- T is a target symmetric tensor, typically expressed as

$$T = \sum_{i=1}^d v_i^{\otimes n},$$

with v_i being the i th row of $V = I_d$,

- $\|\cdot\|_*$ denotes a norm (e.g., the Frobenius norm or a Gaussian norm).

Invariance Under Permutations

In both settings, the loss function is invariant under the action of the group

$$S_d \times S_d,$$

which acts on a $d \times d$ weight matrix W by independently permuting its rows and columns. Formally, for any $(\pi_1, \pi_2) \in S_d \times S_d$ with corresponding permutation matrices P_{π_1} and P_{π_2} , the action is defined as

$$(\pi_1, \pi_2) \cdot W = P_{\pi_1} W P_{\pi_2}^{-1}. \quad (3)$$

The *stabilizer* (or isotropy group) of a weight matrix W is the subgroup of $S_d \times S_d$ that leaves W invariant.

Empirical Observations

Empirical studies reveal that:

- **ReLU Networks:** For networks with an identity target matrix (which has full isotropy group $\Delta S_d = \{(\pi, \pi) \mid \pi \in S_d\}$), local minima consistently exhibit nontrivial stabilizers. In particular, the observed stabilizers are often conjugate to subgroups such as

$$\Delta S_{d-1} \times \Delta S_1 \quad \text{or} \quad \Delta S_{d-2} \times \Delta S_2,$$

which are maximal proper subgroups of ΔS_d . See Figure 1 for an illustration.

- **Tensor Decomposition:** For the tensor decomposition problem with the target tensor

$$T = \sum_{i=1}^d v_i^{\otimes n},$$

where the v_i 's are the rows of $V = I_d$, all local minima are observed to have stabilizers conjugate to subgroups such as

$$\Delta(S_{d-1} \times S_1) \quad \text{or} \quad \Delta(S_{d-3} \times S_2 \times S_1),$$

which are significant subgroups of the isotropy group of V .

These findings suggest that optimization landscapes adhere to a principle of *least symmetry breaking*—while spurious local minima may break the symmetry of the global minimum, they do so minimally. Indeed, after numerous optimization runs (using methods such as gradient descent or Adam), every critical point identified exhibits substantial, nontrivial symmetry.

Kernel Reformulation

Both optimization problems admit an elegant reformulation in terms of kernel functions. Let $\kappa: \mathbb{R}^d \times \mathbb{R}^d \rightarrow \mathbb{R}$ be a kernel function. Then, the loss functions can be expressed as

$$L(W) = \sum_{i,j=1}^d \kappa(w_i, w_j) - 2 \sum_{i,j=1}^d \kappa(w_i, v_j) + \sum_{i,j=1}^d \kappa(v_i, v_j), \quad (4)$$

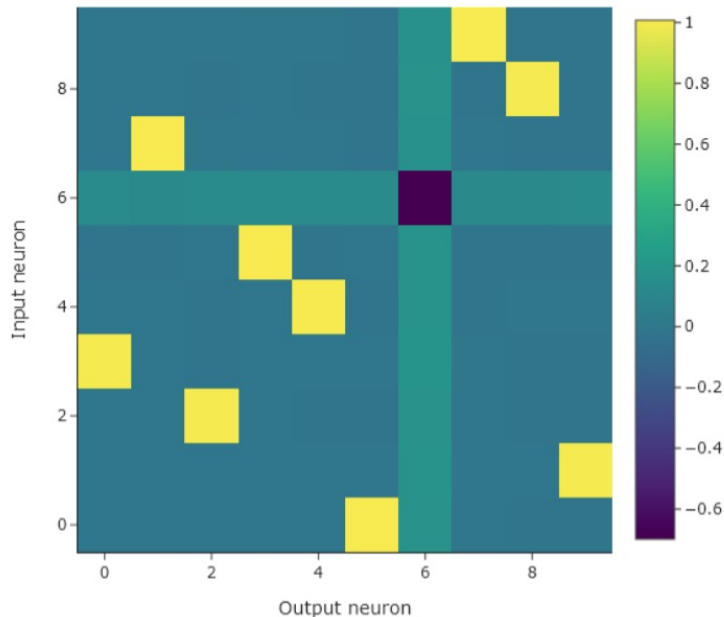


Figure 1: Typical minima observed for ReLU networks with an identity target matrix. The stabilizer under the $S_d \times S_d$ action is conjugate to ΔS_{d-1} .

where w_i and v_i denote the i th rows of W and V , respectively.

For the ReLU network case with $V = I_d$, the corresponding kernel is

$$\kappa_{\text{ReLU}}(w, v) = \mathbb{E}_{x \sim \mathcal{N}(0, I_d)} \left[\phi(w \cdot x) \phi(v \cdot x) \right]. \quad (5)$$

For the tensor decomposition problem under the Frobenius norm, the kernel is given by

$$\kappa_{\text{tensor}}(w, v) = \langle w^{\otimes n}, v^{\otimes n} \rangle_F = \langle w, v \rangle^n, \quad (6)$$

where $\langle \cdot, \cdot \rangle_F$ denotes the Frobenius inner product and $\langle \cdot, \cdot \rangle$ is the standard Euclidean inner product.

1.1 Main results of this paper

Previous research has examined the loss function on shallow ReLU network and tensor decomposition optimization problem. Both are invariant under the $S_d \times S_d$ group action. A key finding was that for these loss functions, every observed local minimum exhibits substantial, nontrivial symmetry through its stabilizer group. In this work, we extend this investigation to several new entirely different symmetry groups.

Projective Space Case

We begin by examining the projective linear group over a finite field $\text{PGL}(n+1, \mathbb{F}_q)$, where n is the dimension of the projective space and q is a prime number. This group acts naturally on the projective space $\mathbb{P}^n(\mathbb{F}_q)$.

We assign a real-valued function to the projective space and define a loss function that remains invariant under the induced action of $\text{PGL}(n+1, \mathbb{F}_q)$ on the space of real-valued functions. The loss function is constructed by summing pairwise interactions (kernel function) between restrictions of the real-valued function on pairs of projective hyperplanes. We initialize the system and optimize the loss function. After optimization, we analyze the stabilizer (denoted as I_V) of the resulting configuration to understand which symmetries are preserved. Our experiments across a wide range of dimensions n , polynomial degree d of the kernel function, and prime numbers q demonstrate that local minima of this loss function consistently possess non-trivial stabilizer subgroups of $\text{PGL}(n+1, \mathbb{F}_q)$.

Graph-Based Cases

We investigate two specific graph structures:

- **Octahedral Graph:** A 6-vertex, 12-edge undirected graph representing an octahedron
- **Perfect Matching Graph:** An undirected perfect matching graph

Though these graphs are undirected, we treat them as directed by assigning two directed edges (i, j) and (j, i) for each undirected edge $\{i, j\} \in E$. The symmetry group acting on each graph consists of its automorphisms, i.e. bijections of the vertex set that preserve the edge structure.

For each vertex i we assign a real value v_i , then for each directed edge $e = (i_1, i_2)$, we define an edge vector (v_{i_1}, v_{i_2}) . We then construct the loss function as the sum of a kernel function evaluated on all pairs of these edge vectors. This kernel function represents the interaction between edges.

We initialize the system and optimize the loss function. After optimization, we analyze the stabilizer (denoted as I_V) of the resulting configuration to understand which symmetries are preserved. Notably, we show that in both graph cases, every observed critical point demonstrates non-trivial, substantial symmetry.

Particle Attraction Case

Finally, we explore a system of n particles in \mathbb{R}^2 . In this model, a kernel function defines the attraction and repulsion between particle pairs, and the overall loss aggregates all pairwise interactions. This loss function is invariant under the action of the symmetric group S_n on particle positions. Our experiments show that almost all critical points possess non-trivial symmetry.

New Measure of Symmetry

To capture more subtle symmetry properties, we introduce a new measure called the **edge isotropy group** (I_E). This group generalizes the vertex isotropy group I_V by identifying all permutations of particles that preserve kernel interactions between pairs. Our results demonstrate that I_E reveals additional symmetry structures not captured by I_V alone.

We demonstrate this by showing that even in the few cases in the particle attraction model where I_V symmetry is trivial, non-trivial I_E symmetry exists. Furthermore, we introduce kernel functions with repulsive terms $1/d^2$ (where d is distance between particles) that force I_V symmetry to be trivial, and we show that they still maintain non-trivial I_E symmetry, demonstrating the power of the I_E measure.

2 Optimization on the Projective Space

2.1 Introduction

Projective spaces are fundamental geometric objects that arise by considering directions rather than points in a vector space. Formally, for a given field F , the n -dimensional projective space $\mathbb{P}^n(F)$ is defined as the set of all one-dimensional subspaces (i.e., lines through the origin) in F^{n+1} . In other words,

$$\mathbb{P}^n(F) = (F^{n+1} \setminus \{0\}) / \sim,$$

where

$$x \sim y \text{ if and only if } \exists \lambda \in F^\times \text{ such that } y = \lambda x.$$

For example, the projective line $\mathbb{P}^1(\mathbb{R})$ consists of all lines through the origin in \mathbb{R}^2 and can be identified with the extended real line $\mathbb{R} \cup \{\infty\}$.

The symmetries of projective spaces are captured by the projective general linear group, denoted $\text{PGL}(n+1, F)$. This group is defined as the quotient

$$\text{PGL}(n+1, F) = \frac{\text{GL}(n+1, F)}{F^\times},$$

where $\text{GL}(n+1, F)$ is the group of all invertible $(n+1) \times (n+1)$ matrices over F and F^\times is the multiplicative group of nonzero elements in F . The quotient removes the ambiguity of scalar multiples, ensuring that each element of $\text{PGL}(n+1, F)$ corresponds to a well-defined transformation on the set of lines. This group naturally acts on $\mathbb{P}^n(F)$ by sending a point (a line)

$$[x_0 : x_1 : \cdots : x_n]$$

to

$$g \cdot [x_0 : x_1 : \cdots : x_n] = \left[g \begin{pmatrix} x_0 \\ x_1 \\ \vdots \\ x_n \end{pmatrix} \right],$$

which is well-defined because any scalar multiple in g cancels out in the projective coordinates.

2.2 Loss Definition

In this section, we explore high-symmetry phenomena in critical points by defining a loss function that is invariant under the projective general linear group $G = \text{PGL}(n+1, \mathbb{F}_q)$, where \mathbb{F}_q is a finite field. Consider the canonical embedding

$$i : \mathbb{P}^{n-1}(\mathbb{F}_q) \hookrightarrow \mathbb{P}^n(\mathbb{F}_q), \quad i(x) = [x : 0].$$

Let \mathcal{F}_m denote the space of real-valued functions on $\mathbb{P}^m(\mathbb{F}_q)$. The group G acts on \mathcal{F}_m by

$$(g \cdot f)(x) = f(g^{-1}x), \quad \forall f \in \mathcal{F}_m, g \in G.$$

We define the restriction map $r : \mathcal{F}_n \rightarrow \mathcal{F}_{n-1}$ as

$$r(f)(x) = f(i(x)), \quad \forall x \in \mathbb{P}^{n-1}(\mathbb{F}_q).$$

Endow \mathcal{F}_{n-1} with the inner product

$$\langle f, g \rangle = \sum_{x \in \mathbb{P}^{n-1}(\mathbb{F}_q)} f(x)g(x),$$

and define the kernel

$$\kappa(f, g) = \langle f, g \rangle^d,$$

for a fixed $d \in \mathbb{N}$.

The loss function $L : \mathcal{F}_n \rightarrow \mathbb{R}$ is then defined as

$$\begin{aligned} L(f) &= \sum_{g_1, g_2 \in G} \kappa(r(g_1 \cdot f), r(g_2 \cdot f)) \\ &\quad - 2 \sum_{g_1, g_2 \in G} \kappa(r(g_1 \cdot f), r(g_2 \cdot 1)) \\ &\quad + \sum_{g_1, g_2 \in G} \kappa(r(g_1 \cdot 1), r(g_2 \cdot 1)), \end{aligned} \tag{7}$$

where 1 denotes the constant function on $\mathbb{P}^n(\mathbb{F}_q)$. For even d , the loss satisfies $L(f) \geq 0$ and attains its global minimum precisely when $f \equiv \pm 1$.

2.3 Results

We conducted experiments by varying three key parameters: the dimension of the projective space, the finite field, and the degree of the kernel (i.e., half of the degree of the polynomial). For every configuration of these parameters, we define a loss function and then initialize numerous points and apply either gradient descent or Newton's method to converge to a critical point. We then analyze the stabilizer of this critical point.

For example, in the projective plane ($n = 2$), we considered finite fields with 2, 3, 5, 7, and 11 elements. In these settings, we achieved convergence for all even-degree kernels ranging from 4 up to 14; furthermore, for the field with 2 elements, we also obtained convergence for kernels of degrees 50 and 100.

Similarly, in the three-dimensional projective space ($n = 3$), our experiments over fields with 2 and 3 elements—for every even-degree kernel between 4 and 12—always revealed the symmetry phenomenon. In the case of four-dimensional projective spaces ($n = 4$), we observed convergence over the field with 2 elements for kernels of degrees 4 to 14.

In all these experiments, most of the minima have fixed value on a projective hyperplane. Therefore the stabilizer at these critical points contains a substantial subgroup of permutations that move this hyperplane to itself. The points identified using Newton’s method occasionally exhibited slightly reduced symmetry, but the overall pattern is clear: every critical point we observed possesses nontrivial symmetry. We refer to Table 10 in the Appendix for the detailed results obtained on the projective plane over \mathbb{F}_2 for $n = 2$ and $d = 8$.

2.4 Results For Reformulated Loss

We obtain similar results when considering an alternative formulation of the loss function that avoids using a target function. In this setting, we define a function

$$L : \mathbb{R}^{\mathbb{P}^n(\mathbb{F}_q)} \rightarrow \mathbb{R}$$

by

$$L(f) = \sum_{g_1, g_2 \in G} \kappa(r(g_1 \cdot f), r(g_2 \cdot f)).$$

Here, the kernel function κ is given by

$$\kappa(f, g) = \langle f, g \rangle^d - c \langle f, g \rangle^q,$$

where $c > 0$ is a positive constant, d is an even integer, and q is an integer with $q < d$. As in the previous cases, all the critical points identified by Newton’s method and GD exhibit nontrivial symmetry.

3 Optimization on the Octahedral Graph

3.1 Loss Definition

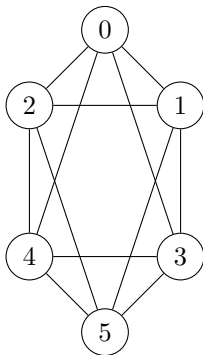


Figure 2: Octahedral Graph

We study the octahedral graph, a 6-vertex, 12-edge undirected graph representing an octahedron. Let $G = (V, E)$ be a graph with vertex set

$$V = \{0, 1, 2, 3, 4, 5\},$$

and edge set:

$$E = \{\{0, 1\}, \{0, 2\}, \{0, 3\}, \{0, 4\}, \{1, 2\}, \{1, 3\}, \{1, 5\}, \{2, 4\}, \{2, 5\}, \{3, 4\}, \{3, 5\}, \{4, 5\}\}.$$

A *graph configuration* is a function $v : V \rightarrow \mathbb{R}$, assigning a value v_i to each vertex i . For each directed edge (i, j) , the corresponding *edge configuration* is

$$a_{ij} = (v_i, v_j).$$

The loss function is defined by

$$L = \sum_{(i,j) \in E} \sum_{(k,l) \in E} \kappa(a_{ij}, a_{kl}),$$

where κ is a bounded-below polynomial kernel function.

We also define the *vertex isotropy group* as

$$I_V(v) = \{\sigma \in \text{Aut}(G) \mid v(\sigma(i)) = v_i \text{ for all } i \in V\}.$$

Kernel Function

In our experiments, we use the kernel

$$\kappa(\mathbf{a}, \mathbf{b}) = (\langle \mathbf{a}, \mathbf{b} \rangle)^p - c (\langle \mathbf{a}, \mathbf{b} \rangle)^q,$$

with the standard inner product $\langle \mathbf{a}, \mathbf{b} \rangle = a_1 b_1 + a_2 b_2$, and parameters $p = 6$, $q = 4$, and $c = 7$.

3.2 Results

Gradient Descent Results

In our experiments, GD always converged to configurations where all vertex values are equal or where one vertex differs from the others:

- All vertex values equal:

$$\text{Loss} = -29269.0$$

$$v_0 = v_1 = v_2 = v_3 = v_4 = v_5 = 1.0393$$

- One vertex differs:

$$v_0 = -1.0393, \quad v_1 = v_2 = v_3 = v_4 = v_5 = 1.0393$$

Newton's Method Results

Using Newton's Method for up to 200 times, we identified 8 critical points with varying isotropy groups. The results are summarized in Table 1.

Table 1: **Octahedral Graph** - Critical Points Found Using Newton's Method

Loss	Positions $(v_0, v_1, v_2, v_3, v_4, v_5)$	I_V Order	I_V Group Name
-29269.0	(1.039, 1.039, 1.039, 1.039, 1.039, 1.039)	48	$C_2 \times S_4$
-16261.0	(-1.039, 1.039, -1.039, -1.039, -1.039, -1.039)	8	D_4
-8073.9	(1.399, 0.758, 0.758, -0.315, -0.315, 1.399)	4	C_2^2
-7510.4	(-0.279, 1.425, 0.685, 0.685, 1.425, -0.279)	8	C_2^3
-3225.5	(-0.252, -0.252, -0.252, 1.085, 1.085, 1.085)	6	S_3
-2164.1	(0.929, -0.192, -0.105, 1.436, -0.192, -0.200)	2	C_2
0	(0, 0, 0, 0, 0, 0)	48	$C_2 \times S_4$

Conclusion

As we saw in the matrices and in the projective case on the octahedral graph, both Gradient Descent and Newton's Method always converge to points with non-trivial isotropy groups.

4 Optimization on the Perfect Matching Graph

4.1 Loss Definition

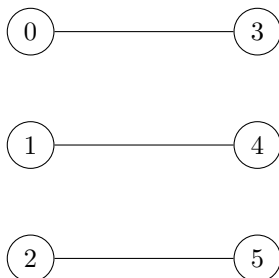


Figure 3: Perfect Matching Graph with $n = 3$

We now shift our focus from the octahedral graph to the *perfect matching graph*. For vectors $\mathbf{a}, \mathbf{b} \in \mathbb{R}^2$, we define the kernel function as

$$\kappa(\mathbf{a}, \mathbf{b}) = \|\mathbf{a} - \mathbf{b}\|^{2p} - c \|\mathbf{a} - \mathbf{b}\|^{2q},$$

where p and q are parameters and c is a constant. The loss function L is then obtained by summing the kernel over all directed edges (i, j) and (k, l) in the edge set E :

$$L = \sum_{(i,j) \in E} \sum_{(k,l) \in E} \kappa(\mathbf{a}_{ij}, \mathbf{a}_{kl}).$$

4.2 Results

To identify graph configurations that minimize L and to study the symmetries preserved in these configurations, we conducted optimization experiments using Gradient Descent (GD) and Newton's Method. The results from Gradient Descent, ordered by the lowest (most negative) loss values, are presented in Table 2.

Gradient Descent Results

The GD results are presented in Table 2, ordered by the lowest (most negative) loss values.

Table 2: **Perfect Matching Graph:** Results for Gradient Descent (GD)

Loss	I_V Order	I_V Group Name	Positions $(v_0, v_1, v_2, v_3, v_4, v_5)$
-1219.6	4	C_2^2	(1.246, -0.174, 0.865, 1.246, 0.865, -0.174)
-914.67	8	D_4	(1.535, 0.115, 0.115, 0.496, 0.115, 0.115)
-813.04	8	D_4	(0.916, 0.916, -0.123, 0.916, 0.916, -0.124)

Newton's Method Results

The critical points found using Newton's Method are presented in Table 3, ordered by the lowest (most negative) loss values.

Table 3: **Perfect Matching Graph:** Results for Newton’s Method

Loss	I_V Order	I_V Group Name	Positions $(v_0, v_1, v_2, v_3, v_4, v_5)$
-534.89	4	C_2^2	$(-0.012, -0.578, 0.848, -0.012, -0.578, -0.198)$
-415.78	2	C_2	$(0.885, 0.321, -0.243, -0.155, 0.321, 0.796)$
-111.02	8	D_4	$(1.172, 0.649, 0.649, 0.126, 0.649, 0.649)$
0.0	48	$C_2 \times S_4$	$(0, 0, 0, 0, 0, 0)$

Conclusion

As we saw in the previous perfect matching case, all the critical points found by Newton’s Method and Gradient Descent have non-trivial isotropy groups.

5 Particle Attraction Case

5.1 Loss Definition

Let $x_1, x_2, \dots, x_n \in \mathbb{R}^2$ be the positions of n particles in the plane.

The kernel function, which represents the interaction between pairs of particles, is given by

$$\kappa(\mathbf{a}, \mathbf{b}) = (\|\mathbf{a} - \mathbf{b}\|^2)^6 - (\|\mathbf{a} - \mathbf{b}\|^2)^4$$

The loss function is given by

$$L = \sum_{i=1}^n \sum_{j=1}^n \kappa(x_i, x_j)$$

5.2 Results

We optimize the loss function for $n = 4$ using Gradient Descent and Newton’s Method to find the critical points. The results are summarized in Table 4.

Table 4: **Particle Attraction Case:** Results for 4 particles for $k = d^{12} - d^8$ kernel

Critical point	Loss	I_V Group Name	I_V Order	Minimum?
1	-1.4815	C_2	2	Yes
2	-1.1852	C_2^2	4	Yes
3	-0.88889	S_3	6	Yes
4	-0.94181	I	1	No
5	-0.91969	I	1	No
6	-0.60196	C_2	2	No
7	-0.3098	C_2	2	No
8	0	S_4	24	No

The corresponding plots for each critical point can be found in Figure 4 in the Appendix.

Observations: The results show that the vertex isotropy group I_V is non-trivial at most of the observed critical points. Later we will see that the only points (number 5, 6) with trivial symmetry have non-trivial edge isotropy group I_E .

We conducted the same experiments with 7 particles. The results summarized in Table 5 show that all the critical points have non-trivial isotropy groups.

Table 5: **Particle Attraction Case:** - Results for 7 particles for $k = d^{12} - d^8$ kernel

Critical point	Loss	I_V Group Name	I_V Order	Minimum?
1	-4.7407	$C_2^2 \times S_3$	24	Yes
2	-4.4444	S_3^2	36	Yes
3	-2.963	$C_2 \times S_5$	240	Yes
4	0	S_7	5040	No
5	-4.1605	D_6	12	No
6	-3.8667	D_6	12	No
7	-3.5771	D_6	12	No
8	-3.0253	C_2^2	4	No
9	-2.9985	C_2^3	8	No
10	-2.9799	S_4	24	No
11	-2.7265	C_2^2	4	No
12	-2.715	S_4	24	No
13	-2.6967	D_6	12	No
14	-2.4711	C_2^2	4	No
15	-2.3891	S_3	6	No
16	-2.1642	C_2^2	4	No
17	-1.8107	C_2	2	No
18	-1.6567	C_2^2	4	No
19	-1.6279	S_3	6	No
20	-1.5994	D_6	12	No
21	-1.5652	C_2^2	4	No
22	-1.4331	C_2	2	No
23	-1.3177	C_2^2	4	No
24	-1.2911	S_3	6	No
25	-1.226	S_3	6	No
26	-1.2107	C_2^2	4	No
27	-0.9973	S_3	6	No
28	-0.92304	S_3^2	36	No
29	-0.63063	$C_2 \times S_4$	48	No
30	-0.33078	S_5	120	No

The corresponding plots for each critical point can be found in Figure 13 in the Appendix.

Observations: All the critical points except two points in the $n = 4$ case, have non-trivial isotropy groups, and most of them have large symmetry. We will see later that the two points with the trivial I_V symmetry have other (I_E) non-trivial symmetry.

5.3 Robustness Under Varying Kernel Functions and High-Degree Polynomials

In our particle attraction experiments, the loss function is generated by a kernel function, which in our initial setup is based on the distance between particles. However, our observations indicate that the resulting behavior is not restricted solely to distance-based kernels. In fact, when we replace the distance with the inner product between particles, and even when considering the inner product raised to high powers (e.g., the inner product to the 50th, resulting in the loss being a polynomial of degree 100), the critical points also always possessed non-trivial high symmetry. In fact, in these cases, the critical points appear as a perturbation of the critical points in lower degree polynomial kernels.

Moreover, it seems that similar phenomena occur when the kernel function is a randomly chosen polynomial. For instance, in the appendix E, we fixed the kernel as a bounded below polynomial of degree 4. Our experiments again reveal that the critical points in those cases always possess large symmetry. This robustness persists regardless of whether the kernel is derived from the distance or from an inner product or perhaps (needs more experiments) from a randomly chosen polynomial.

5.4 Narrow Attraction Basins of Non-Symmetric Minima (if they indeed exist)

In all the cases we have studied—whether it’s the projective plane, the octahedral graph, or the perfect matching case—every local minimum observed exhibited non-trivial symmetry. In those experiments, roughly 1,000 trials per case consistently yielded symmetric minima. To rigorously test the possibility that a non-symmetric minimum might exist, we selected one representative scenario using an inner-product-based kernel powered by 8 (i.e., a 16th-degree polynomial) and ran an extensive series of about 30 million experiments. Not a single one of these runs produced a non-symmetric minimum; all converged to one of the four symmetric minima we had already identified.

This overwhelming evidence suggests that, while we cannot theoretically rule out the existence of non-symmetric minima, if they do exist their basins of attraction must be extraordinarily narrow—so much so that they are effectively undetectable even under exhaustive search. For further details, see Appendix D.

6 New Measure of Symmetry - Edge Isotropy Group I_E

6.1 Introduction

In this section, we will define and demonstrate the importance of the edge isotropy group I_E in capturing symmetries that are not evident from the I_V group alone. We start by examining the edge isotropy group for the particle attraction loss function as defined in the previous section. We showed that the group I_E measures symmetries that the group I_V does not capture in the case of 4 and 7 particles.

6.2 Edge Isotropy Group Definition I_E

Definition 1 (Edge Isotropy Group I_E). *The edge isotropy group $I_E(a)$ consists of automorphisms that preserve the kernel values between edge pairs:*

$$I_E(a) = \{ \sigma \in \text{Aut}(G) \mid k(\mathbf{a}_{\sigma(i)\sigma(j)}, \mathbf{a}_{\sigma(k)\sigma(l)}) = k(\mathbf{a}_{ij}, \mathbf{a}_{kl}) \quad \forall (i, j), (k, l) \in E \}$$

Obviously we have the relation $I_V \subset I_E$, because each permutation that fixes the vertex values also fixes the kernel values between edges. However, as we will see in the following examples, the edge isotropy group I_E in many cases is larger than the vertex isotropy group I_V .

6.3 I_E Isotropy Group for $n = 4$, $n = 7$ ($\kappa(x, y) = \|x - y\|^{12} - \|x - y\|^8$ kernel)

We begin by presenting the previous tables for 4 and 7 particles experiments. We have added a column of the edge isotropy group I_E and its order.

The extended results for $n = 4$ are summarized in Table 6.

Table 6: Extended table with I_E groups, $n = 4$, $\kappa(x, y) = \|x - y\|^{12} - \|x - y\|^8$ kernel

Critical point	Loss	I_V Group Name	I_V Order	I_E Group Name	I_E Order	Minimum?
1	-1.4815	C_2	2	C_2^2	4	Yes
2	-1.1852	C_2^2	4	D_4	8	Yes
3	0	S_4	24	S_4	24	No
4	-0.94181	I	1	C_2	2	No
5	-0.91969	I	1	S_3	6	No
6	-0.60196	C_2	2	C_2	2	No
7	-0.3098	C_2	2	C_2^2	4	No
8	-0.88889	S_3	6	S_3	6	Yes

The corresponding plots for each critical point can be found in Figure 4 in the Appendix.

The extended results for $n = 7$ are summarized in Table 7.

Table 7: Extended table with I_E groups, $n = 7$, $\kappa(x, y) = \|x - y\|^{12} - \|x - y\|^8$ kernel

Critical point	Loss	I_V Group Name	I_V Order	I_E Group Name	I_E Order	Minimum?
1	-4.7407	$C_2^2 \times S_3$	24	$D_4 \times S_3$	48	Yes
2	-4.4444	S_3^2	36	$(S_3^2 \times C_2)$	72	Yes
3	-2.963	$C_2 \times S_5$	240	$C_2 \times S_5$	240	Yes
4	0	S_7	5040	S_7	5040	No
5	-4.1605	D_6	12	D_6	12	No
6	-3.8667	D_6	12	D_6	12	No
7	-3.5771	D_6	12	D_6	12	No
8	-3.0253	C_2^2	4	C_2^2	4	No
9	-2.9985	C_2^3	8	$C_2 \times D_4$	16	No
10	-2.9799	S_4	24	S_4	24	No
11	-2.7265	C_2^2	4	C_2^3	8	No
12	-2.715	S_4	24	$C_2 \times S_4$	48	No
13	-2.6967	D_6	12	D_6	12	No
14	-2.4711	C_2^2	4	D_4	8	No
15	-2.3891	S_3	6	S_3	6	No
16	-2.1642	C_2^2	4	C_2^3	8	No
17	-1.8107	C_2	2	C_2^2	4	No
18	-1.6567	C_2^2	4	D_4	8	No
19	-1.6279	S_3	6	S_3	6	No
20	-1.5994	D_6	12	$C_2^2 \times S_3$	24	No
21	-1.5652	C_2^2	4	C_2^3	8	No
22	-1.4331	C_2	2	C_2^2	4	No
23	-1.3177	C_2^2	4	C_2^2	4	No
24	-1.2911	S_3	6	D_6	12	No
25	-1.226	S_3	6	$C_2^2 \times S_3$	24	No
26	-1.2107	C_2^2	4	C_2^3	8	No
27	-0.9973	S_3	6	D_6	12	No
28	-0.92304	S_3^2	36	S_3^2	36	No
29	-0.63063	$C_2 \times S_4$	48	$C_2 \times S_4$	48	No
30	-0.33078	S_5	120	$C_2 \times S_5$	240	No

The corresponding plots for each critical point can be found in Figure 13 in the Appendix.

Observations: We can see that the edge isotropy group I_E is consistently larger than the vertex isotropy group I_V in the experiments. Furthermore, in the case of 4 particles, for the 5, 6 critical points, the vertex isotropy group I_V is trivial, but the edge isotropy group I_E is non-trivial.

6.4 Experiments for $n = 4$ and $n = 7$ with $\kappa = \|\mathbf{a} - \mathbf{b}\|^2 + \frac{1}{\|\mathbf{a} - \mathbf{b}\|^2}$ Kernel

The power of I_E and the idea that it generalizes the symmetries in I_V is reflected in the experiments where our kernel function is given by:

$$\kappa(\mathbf{a}, \mathbf{b}) = \begin{cases} \|\mathbf{a} - \mathbf{b}\|^2 + \frac{1}{\|\mathbf{a} - \mathbf{b}\|^2}, & \text{if } \mathbf{a} \neq \mathbf{b} \\ 0, & \text{if } \mathbf{a} = \mathbf{b} \end{cases}$$

In this case, the vertex isotropy group I_V is trivial (I_V order = 1) for all experiments, as expected due to the repulsion term $\frac{1}{\|\mathbf{a} - \mathbf{b}\|^2}$ in the kernel. However, the edge isotropy group I_E is non-trivial, indicating deeper symmetries in the edge interactions.

Table 8: Results for $n = 4$ ($d^2 + \frac{1}{d^2}$ Kernel function)

Critical point	Loss	I_V Group Name	I_V Order	I_E Group Name	I_E Order	Minimum?
1	25.298	I	1	D_4	8	Yes
2	27.708	I	1	C_2	2	No
3	33.941	I	1	C_2	2	No

The corresponding plots for each critical point can be found in Figure 44 in the Appendix.

And here is results for the same kernel for $n = 7$:

Table 9: Results for $n = 7$ ($d^2 + \frac{1}{d^2}$ Kernel function)

Critical point	Loss	I_V Group Name	I_V Order	I_E Group Name	I_E Order	Minimum?
1	99.559	I	1	D_6	12	Yes
2	102.97	I	1	C_2	2	No
3	103.15	I	1	C_2	2	No
4	103.35	I	1	C_2	2	No
5	104.77	I	1	D_7	14	No
6	105.95	I	1	C_2	2	No
7	109.12	I	1	C_2	2	No
8	113.02	I	1	C_2^2	4	No
9	114.91	I	1	C_2	2	No
10	121.85	I	1	C_2	2	No
11	131.51	I	1	C_2	2	No
12	157.15	I	1	C_2	2	No

The corresponding plots for each critical point can be found in Figure 48 in the Appendix.

Observations: Similar to the $n = 4$ case, while I_V is trivial, I_E remains non-trivial.

6.5 Summary of the Edge Isotropy Group I_E

In this section, we introduced the edge isotropy group I_E , which generalizes the vertex isotropy group I_V by identifying more complex symmetry structures in optimization landscapes. Through our experiments with particle attraction cases involving 4 and 7 particles, we found that I_E consistently captures symmetries that I_V alone does not detect. Notably, several scenarios exhibited trivial I_V groups while revealing non-trivial I_E groups, highlighting deeper symmetries embedded within edge interactions.

Furthermore, this observation remained valid even for kernels explicitly containing repulsive terms designed to eliminate vertex-level symmetries. Such findings underscore the robustness and importance of the I_E group as an analytical tool. The consistent observation that I_E is larger than I_V across various configurations suggests that I_E is a promising generalization of symmetry measurement. Ultimately, this generalized symmetry measure can enable a broader exploration of symmetry phenomena, potentially uncovering the underlying mechanisms that drive symmetry in critical points.

7 Summary

In this work, we investigate symmetry phenomena in a range of optimization settings by examining the isotropy groups of the critical points. Building on earlier studies in ReLU networks and symmetric tensor decomposition, we consider four distinct cases: the projective space over finite fields, the octahedral graph, the perfect matching graph, and the particle attraction model. In each scenario, both gradient descent and Newton’s method always converge to local minima that exhibit substantial non-trivial symmetry. Moreover, our experiments show that even when varying the kernel functions or employing high-degree polynomial kernels, the optimization process always converges to points with non-trivial symmetry, indicating that the

basins of attraction for any non-symmetric minima (if they indeed exist) are negligibly small. To capture subtle symmetries that are not revealed by vertex configurations alone, we finally introduce the *Edge Isotropy Group* (I_E). This additional metric provides deeper insight into the symmetric structure of the minima of loss landscapes and reinforces the principle of least symmetry breaking observed throughout our experiments. Detailed experimental data and further analyses supporting these findings are presented in the Appendix.

Acknowledgements

I would like to express my sincere gratitude to David Kazhdan, Yossi Arjevani, and Shmuel Weinberger for their invaluable guidance and insightful discussions throughout this work.

Appendix

A Detailed Experimental Data for the Projective Plane over the Field \mathbb{F}_2

In this appendix, we present detailed experimental data for the projective plane over the field \mathbb{F}_2 . Let $v \in \mathcal{F}_n$ and denote

$$\begin{aligned} v_1 &= v((0, 0, 1)), & v_2 &= v((0, 1, 0)), & v_3 &= v((0, 1, 1)), \\ v_4 &= v((1, 0, 0)), & v_5 &= v((1, 0, 1)), & v_6 &= v((1, 1, 0)), & v_7 &= v((1, 1, 1)). \end{aligned}$$

Table 10: Critical points Data for Field \mathbb{F}_2 and Polynomial Degree 16

Loss	Weights	I_V (stabilizer group) Order	I_V Group Name
0	$v_1 v_2 v_3 v_4 v_5 v_6 v_7 = 1.0$	168	$\text{PGL}(3, 2)$
21079.60	$v_1 v_2 = 1.27492$ $v_3 = 1.27494$ $v_4 v_7 = 0.03937$ $v_5 v_6 = -0.03567$	4	$C_2 \times C_2$
21079.610	$v_1 v_2 = 1.27493$ $v_3 = 1.27492$ $v_4 = -0.05162$ $v_5 v_6 = 0.0025$ $v_7 = 0.05402$	2	C_2
21079.615	$v_1 v_2 v_3 = 1.27493$ $v_4 = -0.06263$ $v_5 v_6 v_7 = 0.02335$	6	S_3
21079.616	$v_1 v_2 v_3 = 1.27493$ $v_4 v_6 v_7 = -0.01963$ $v_5 = 0.0663$	6	S_3
21080	$v_1 v_2 v_3 = 1.27493$ $v_4 v_5 v_6 v_7 = 0.0018$	24	S_4
93233	$v_1 v_2 v_3 = 1.2173$ $v_4 v_5 v_6 = 0.82001$ $v_7 = -0.10076$	6	S_3
104452	$v_1 v_2 v_3 = 1.24105$ $v_4 v_5 v_6 v_7 = 0.61958$	24	S_4
11306411	$v_1 v_2 v_3 = 0.0$ $v_4 v_5 = 1.09527$ $v_6 v_7 = -1.09527$	4	$C_2 \times C_2$
11528833	$v_1 v_2 = 0.99946$ $v_3 = -0.2527$ $v_4 v_5 v_6 v_7 = -0.67966$	8	D_4
11544284	$v_1 v_2 = 0.7481$ $v_3 = -0.92777$ $v_4 v_7 = -0.34603$ $v_5 = 1.15453$ $v_6 = -0.01432$	2	C_2
11560780	$v_1 v_2 = 0.51586$ $v_3 = -0.46628$ $v_4 = -0.89189$ $v_5 v_6 = 0.91016$ $v_7 = -0.10749$	2	C_2

Table 10 continued

Loss	Weights	I_V Order	I_V Group Name
11564812	$v_1 v_2 v_5 = 0.87152$ $v_3 v_4 v_7 = -0.45644$ $v_6 = -0.08012$	6	S_3
11565260	$v_1 v_2 = 0.29492$ $v_3 = 0.79675$ $v_4 v_5 v_6 v_7 = -0.7562$	8	D_4
11566743	$v_1 v_2 v_6 = 0.61893$ $v_3 v_4 v_7 = -0.44323$ $v_5 = 1.0662$	6	S_3
11567466	$v_1 v_2 = 0.74245$ $v_3 = -0.3452$ $v_4 v_7 = -0.48573$ $v_5 = 0.95005$ $v_6 = 0.54832$	2	C_2
11567945	$v_1 v_2 = 0.83873$ $v_3 = -0.49864$ $v_4 v_7 = 0.68525$ $v_5 v_6 = -0.40378$	4	$C_2 \times C_2$
11568165	$v_1 v_2 v_3 = -0.43366$ $v_4 v_5 v_6 v_7 = 0.76953$	24	S_4
11571824	$v_1 v_2 = 0.60545$ $v_3 = -0.93276$ $v_4 v_7 = -0.07086$ $v_5 = 0.53502$ $v_6 = -0.6828$	2	C_2
11572799	$v_1 v_2 = 0.75893$ $v_3 = -0.57575$ $v_4 v_7 = -0.18882$ $v_5 = 0.35018$ $v_6 = -0.75595$	2	C_2
11573312	$v_1 = 0.85652$ $v_2 v_3 v_4 v_6 v_7 = -0.0$ $v_5 = -0.85652$	4	$C_2 \times C_2$
11573350	$v_1 v_2 = 0.23222$ $v_3 = 0.19656$ $v_4 v_7 = -0.21457$ $v_5 = 0.81487$ $v_6 = -0.86003$	2	C_2
11573387	$v_1 v_2 = 0.33387$ $v_3 = 0.0$ $v_4 v_7 = -0.33387$ $v_5 = -0.81544$ $v_6 = 0.81544$	2	C_2
11573462	$v_1 = 0.93886$ $v_2 = -0.59133$ $v_3 = 0.39297$ $v_4 v_5 v_6 v_7 = -0.0883$	4	$C_2 \times C_2$

Table 10 continued

Loss	Weights	I_V Order	I_V Group Name
11573479	$v_1 v_2 = 0.24957$ $v_3 = -0.42817$ $v_4 v_7 = -0.09292$ $v_5 = -0.89686$ $v_6 = 0.60173$	2	C_2
11573551	$v_1 v_2 = 0.5086$ $v_3 = -0.8155$ $v_4 v_5 v_6 v_7 = 0.06123$	8	D_4
11573569	$v_1 v_2 = 0.60785$ $v_3 = -0.63187$ $v_4 v_5 v_6 v_7 = -0.00935$	8	D_4
11573599	$v_1 = 0.7865$ $v_2 v_3 v_4 v_5 v_6 v_7 = -0.15037$	24	S_4
11573604	$v_1 v_2 v_3 v_4 v_5 v_6 v_7 = -0.0$	168	$\text{PGL}(3, 2)$

B Plots for particle attraction case

B.1 Plots for 4 particles Experiments (kernel $d^{12} - d^8$)

The plots are ordered in the order of the experiments in the table.

Figure 4: Visualization of critical points from Table 4

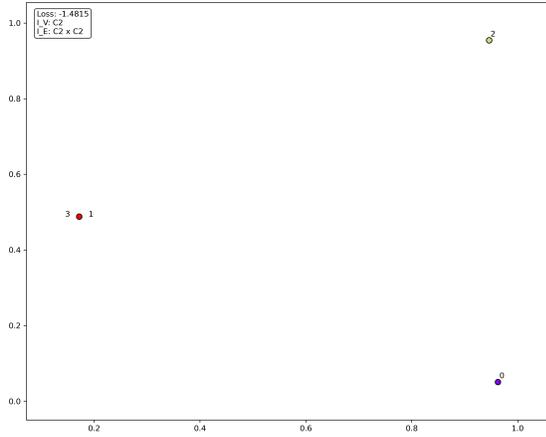


Figure 5

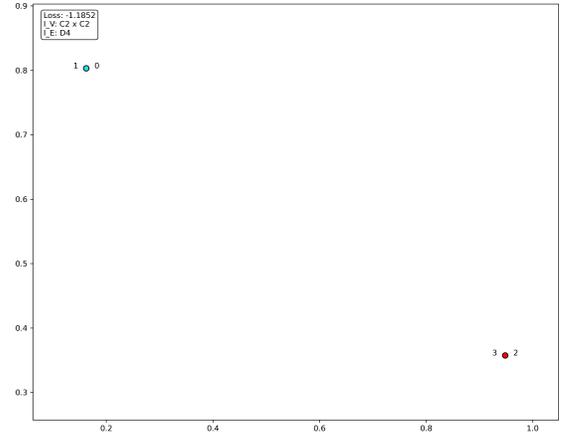


Figure 6

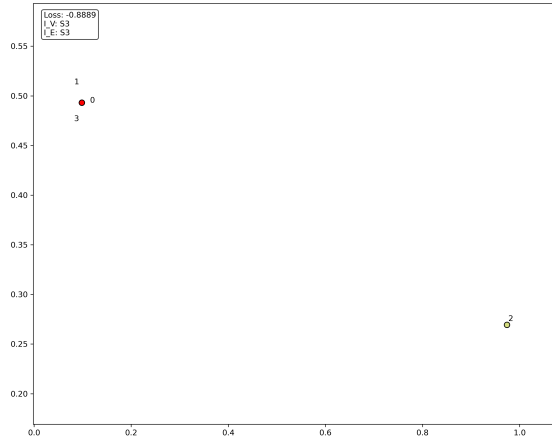


Figure 7

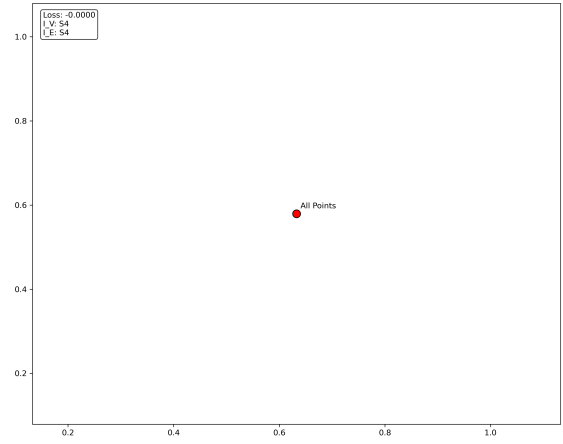


Figure 8

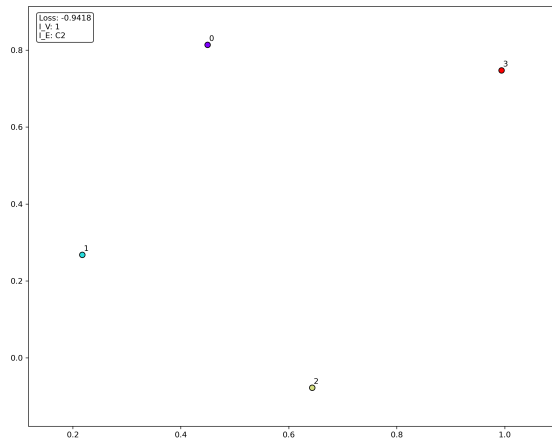


Figure 9

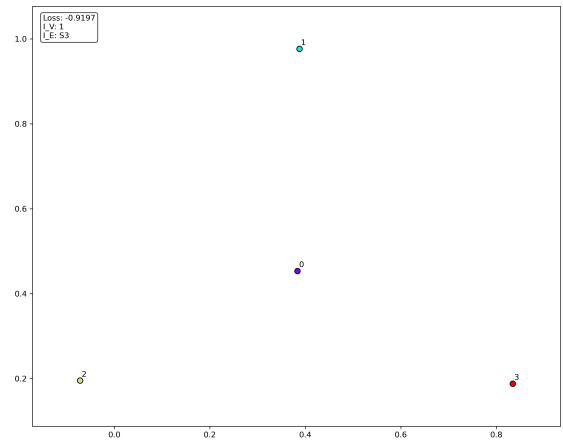


Figure 10

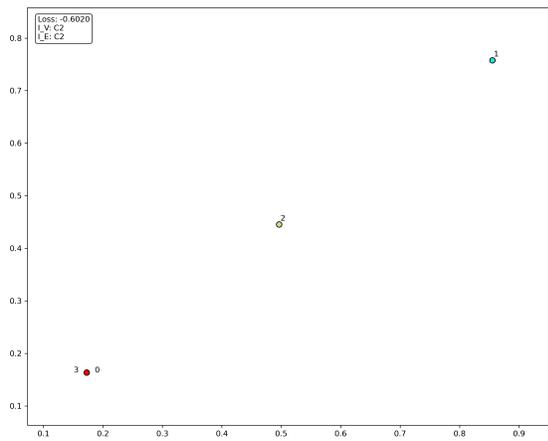


Figure 11

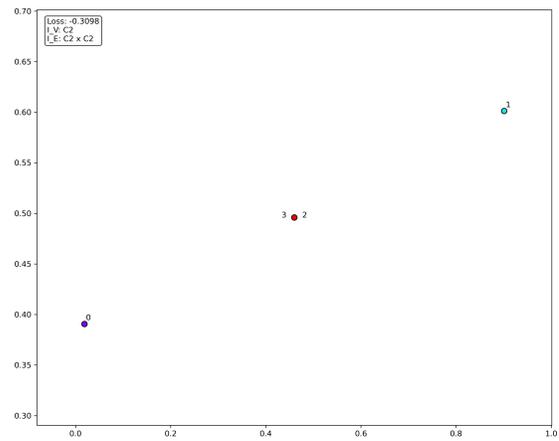


Figure 12

B.2 Plots for 7 particles Experiments (kernel $d^{12} - d^8$)

The plots are ordered in the order of the experiments in the table.

Figure 13: Visualization of critical points from Table 5

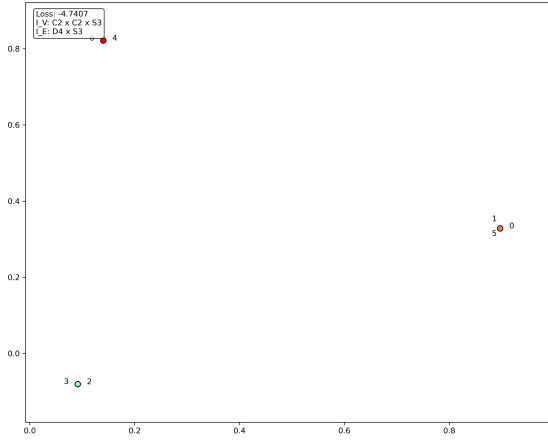


Figure 14

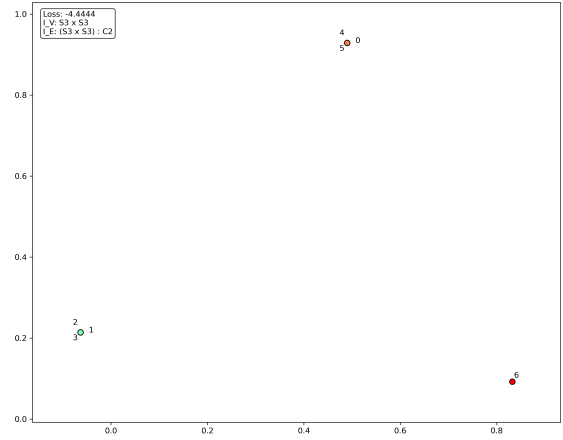


Figure 15

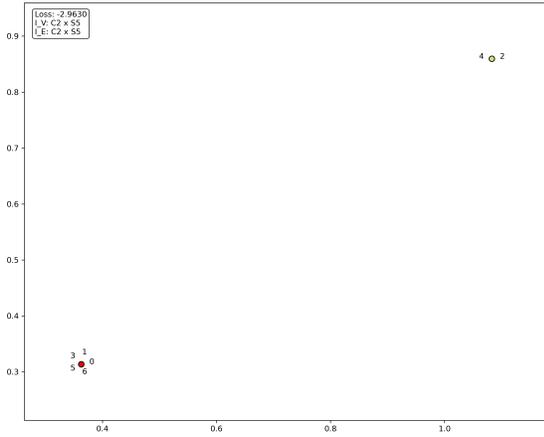


Figure 16

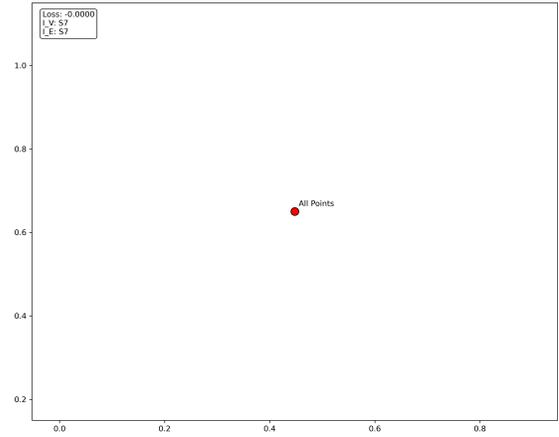


Figure 17

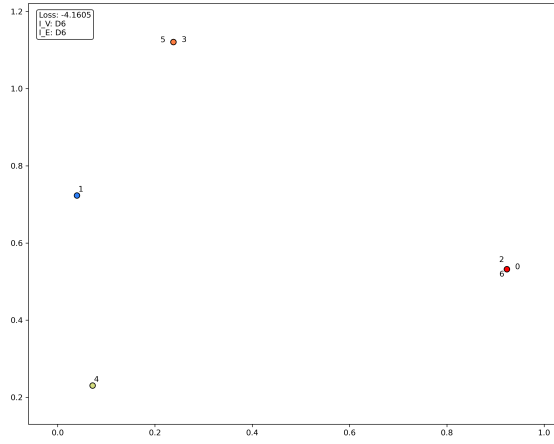


Figure 18

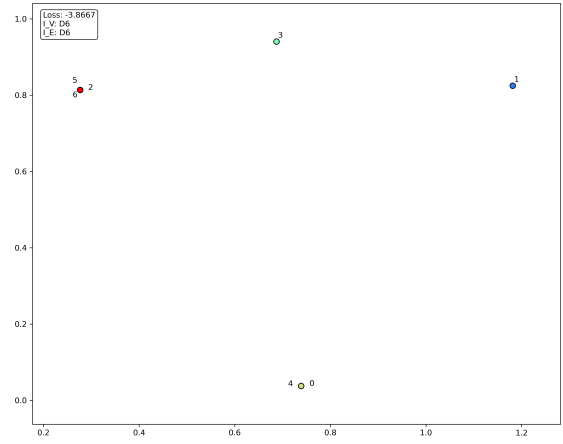


Figure 19

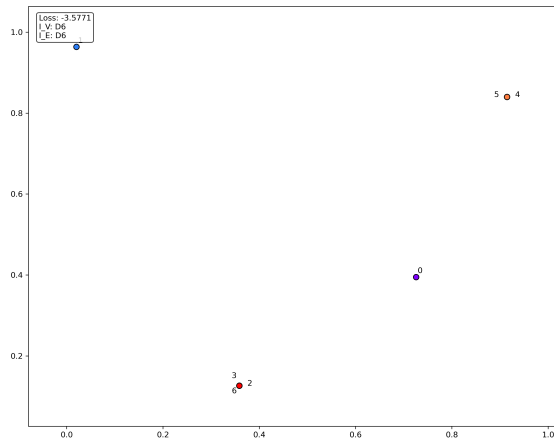


Figure 20

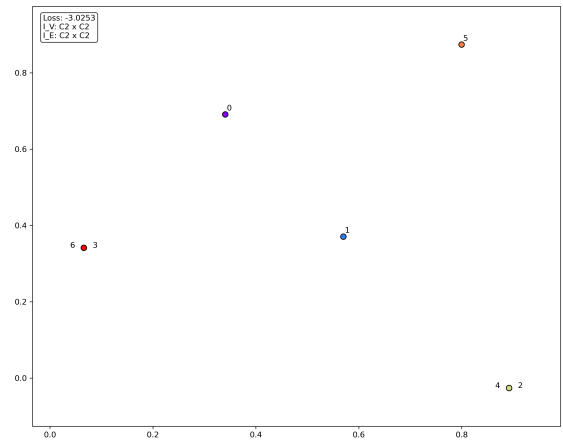


Figure 21

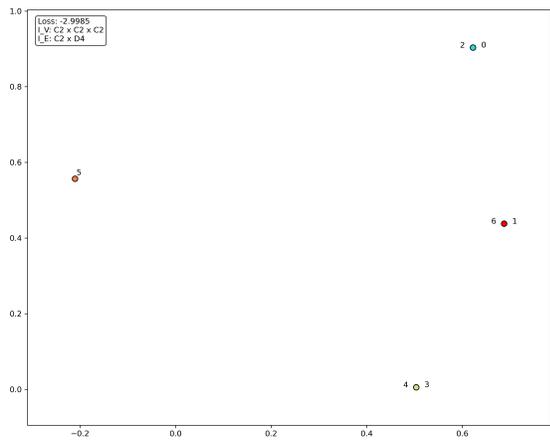


Figure 22

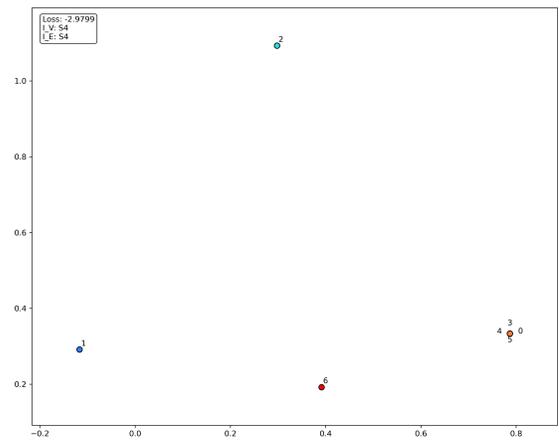


Figure 23

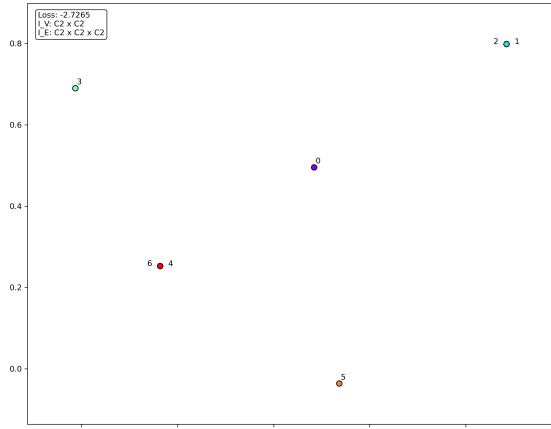


Figure 24

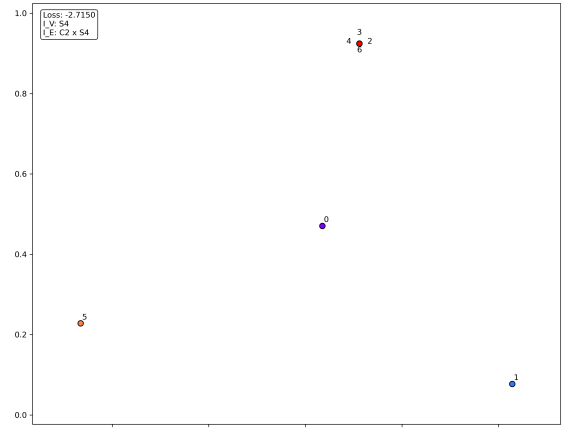


Figure 25

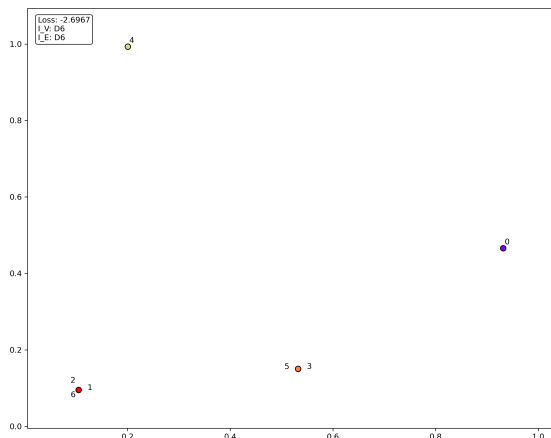


Figure 26

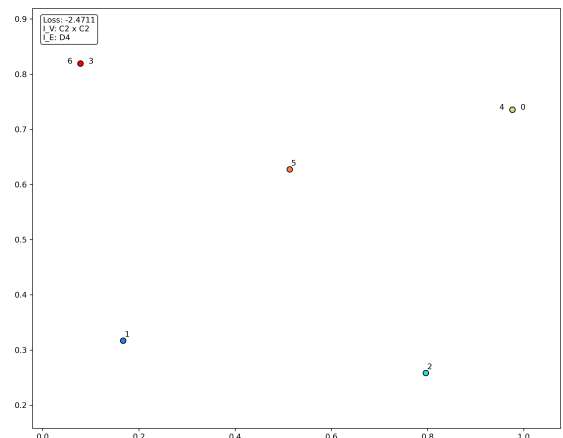


Figure 27

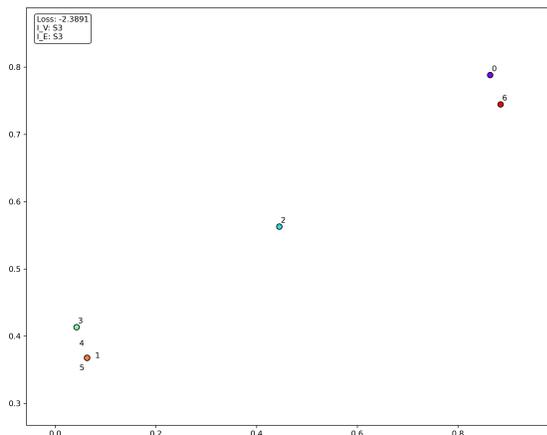


Figure 28

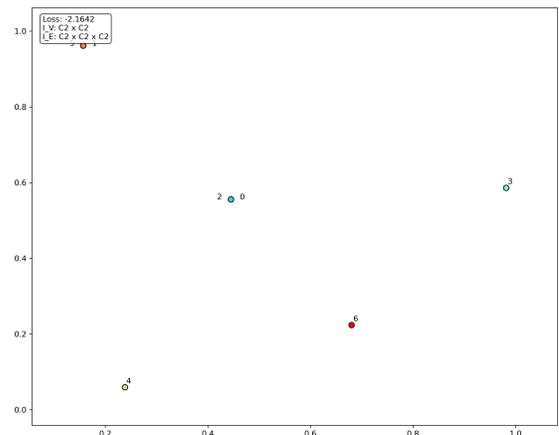


Figure 29

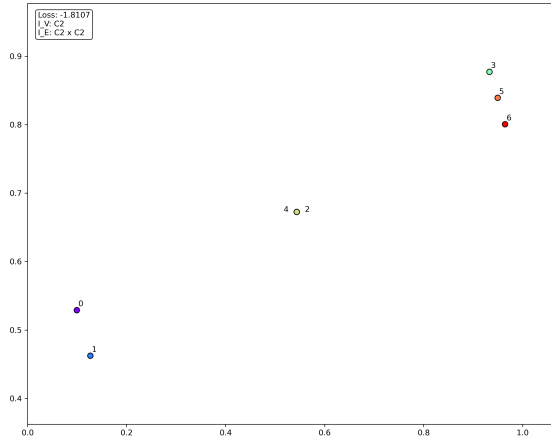


Figure 30

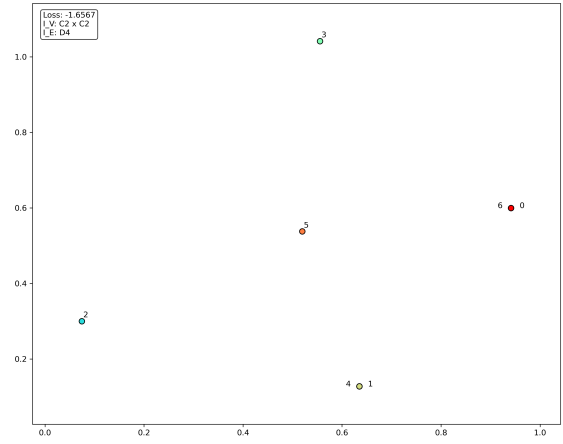


Figure 31

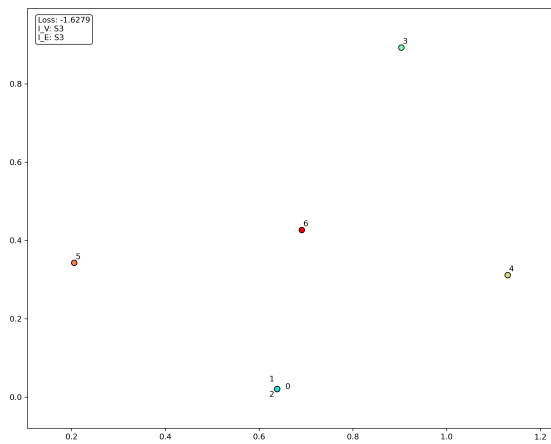


Figure 32

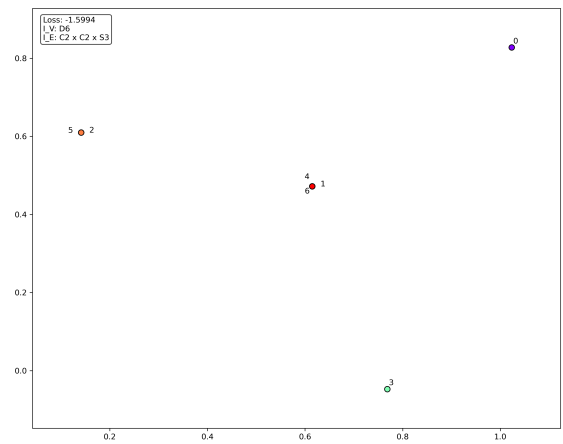


Figure 33

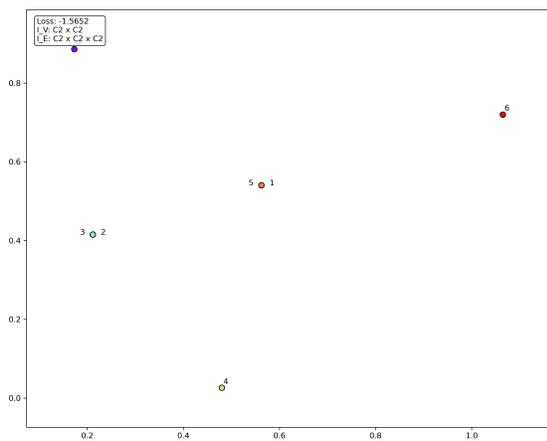


Figure 34

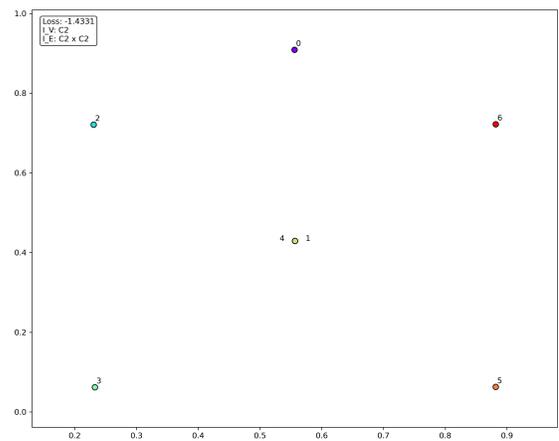


Figure 35

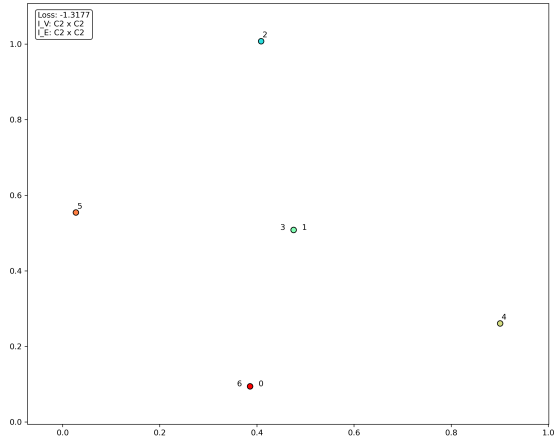


Figure 36

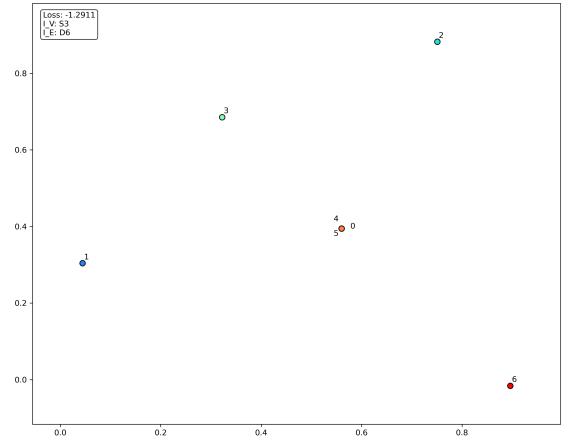


Figure 37

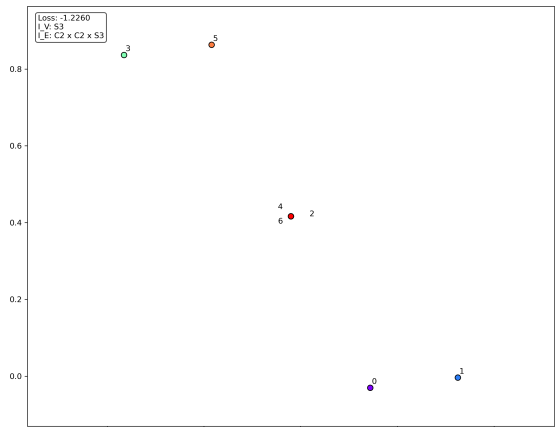


Figure 38

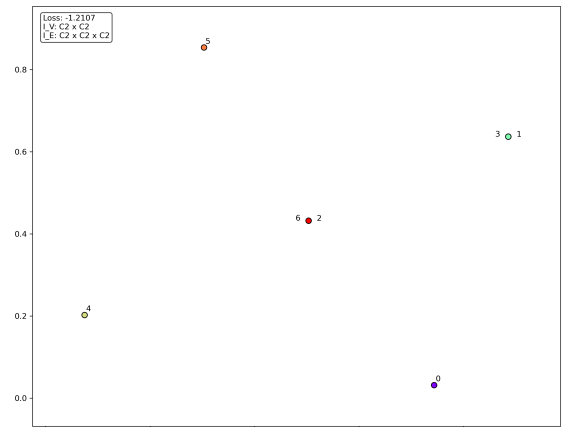


Figure 39

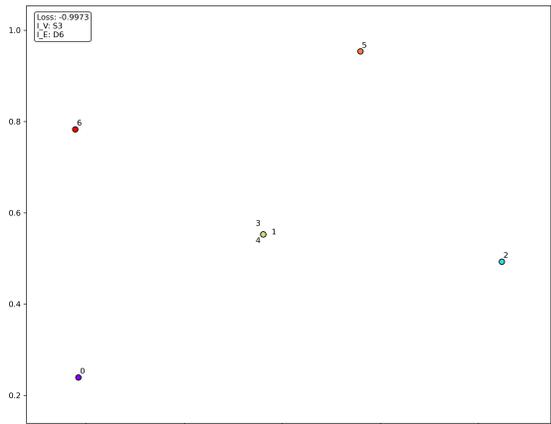


Figure 40

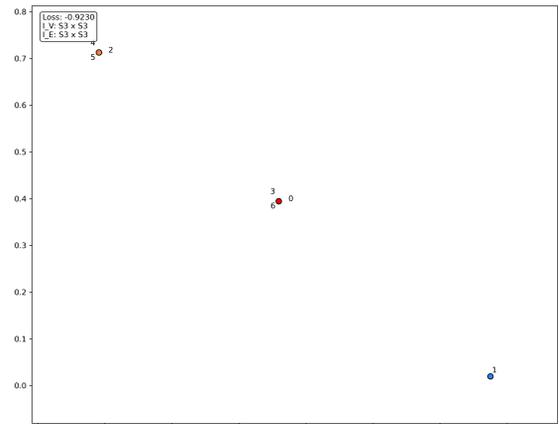


Figure 41

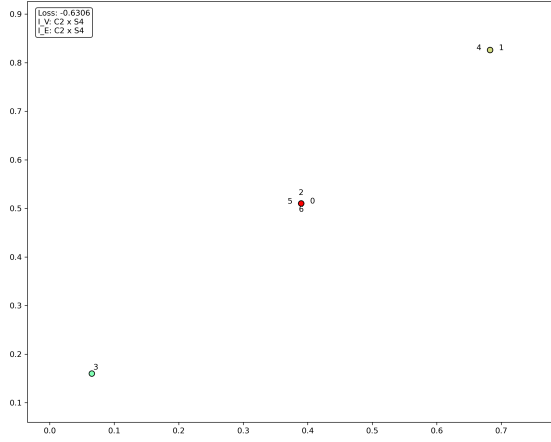


Figure 42

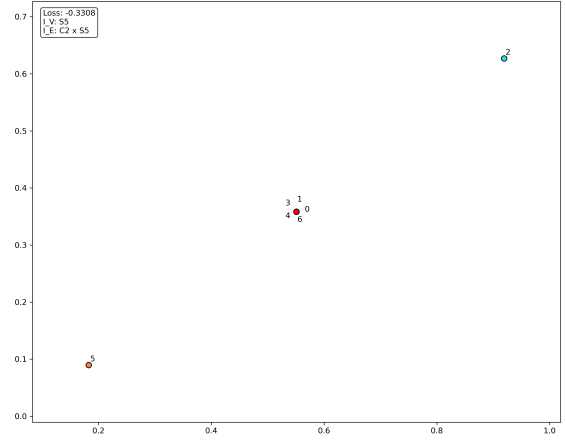


Figure 43

B.3 Plots for 4 particles Experiments (kernel $d^2 + \frac{1}{d^2}$)

The plots are ordered in the order of the experiments in the table.

Figure 44: Visualization of critical points from Table 8

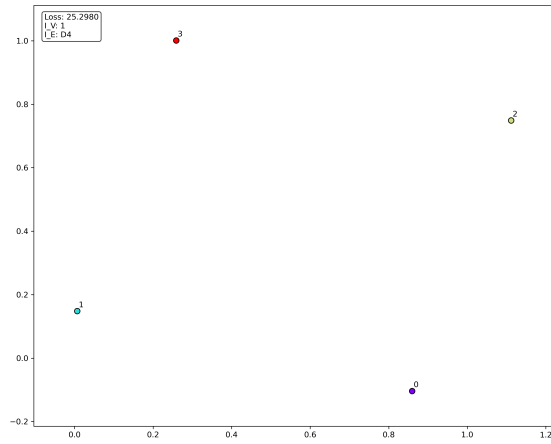


Figure 45

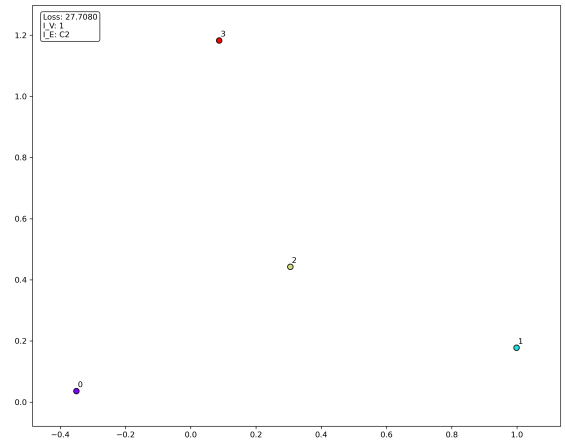


Figure 46

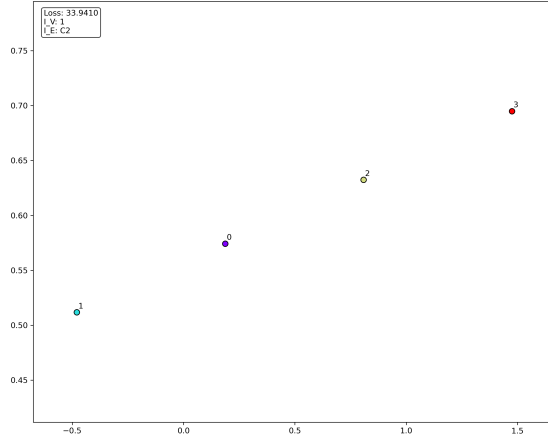


Figure 47

B.4 Plots for 7 particles Experiments (kernel $d^2 + \frac{1}{d^2}$)

The plots are ordered in the order of the experiments in the table.

Figure 48: Visualization of critical points from Table 9

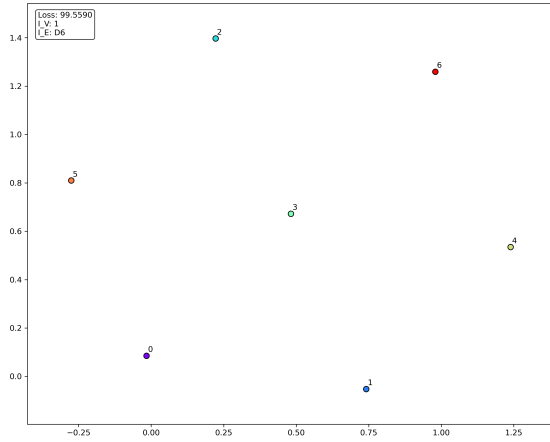


Figure 49

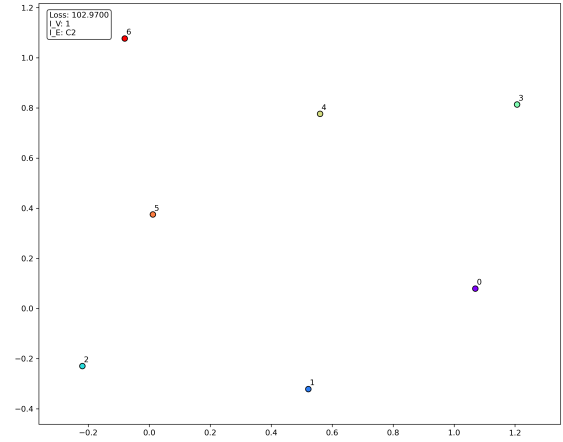


Figure 50

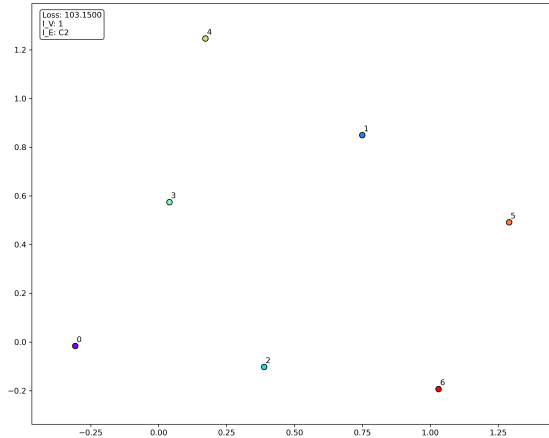


Figure 51

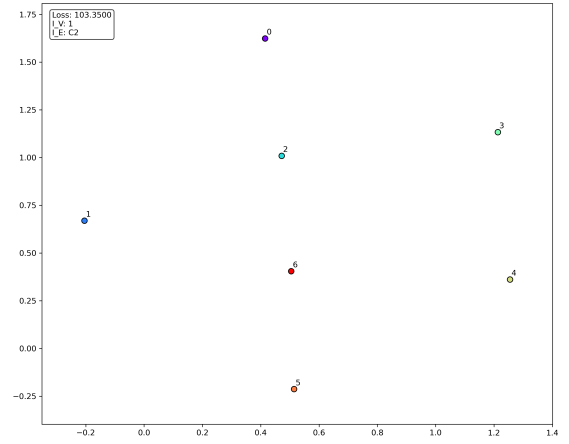


Figure 52

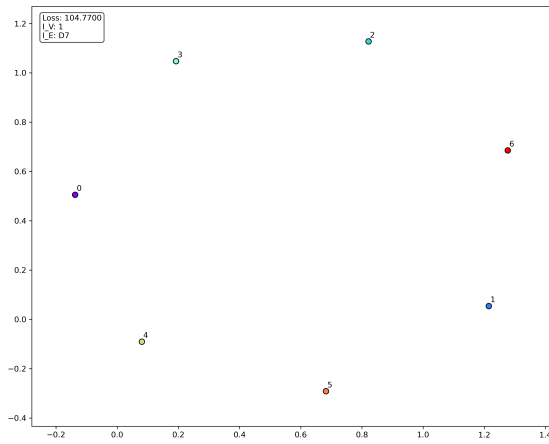


Figure 53

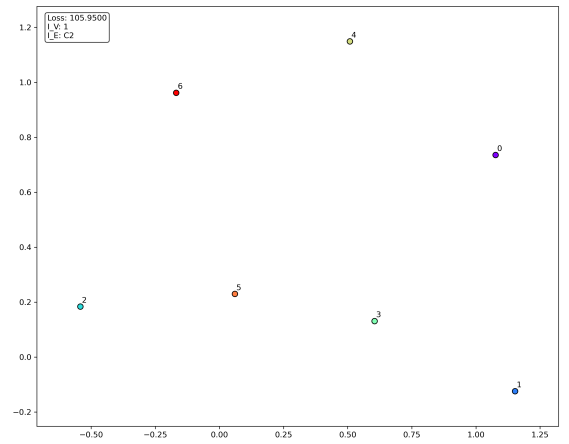


Figure 54

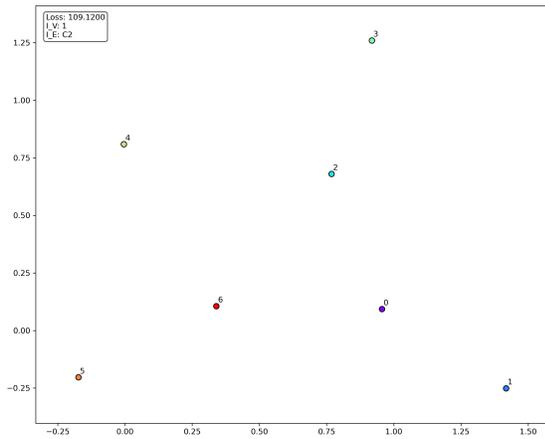


Figure 55

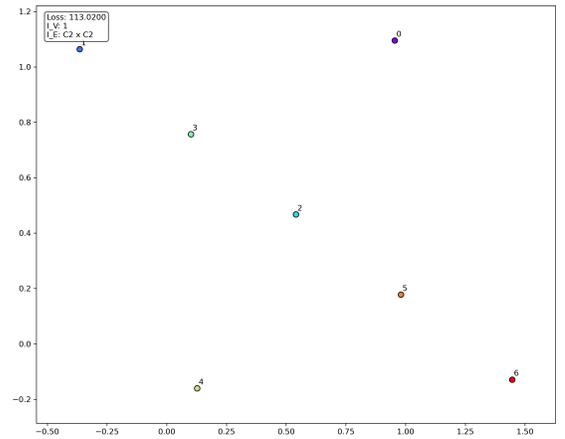


Figure 56

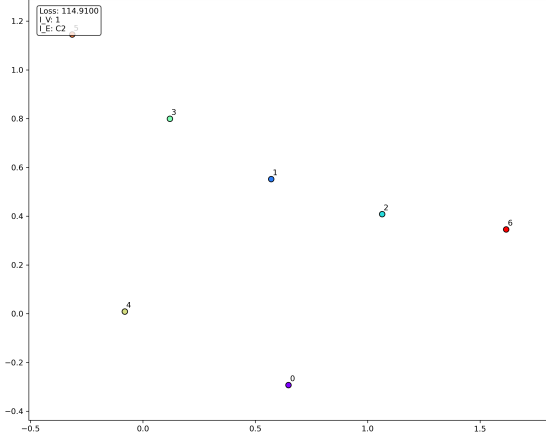


Figure 57

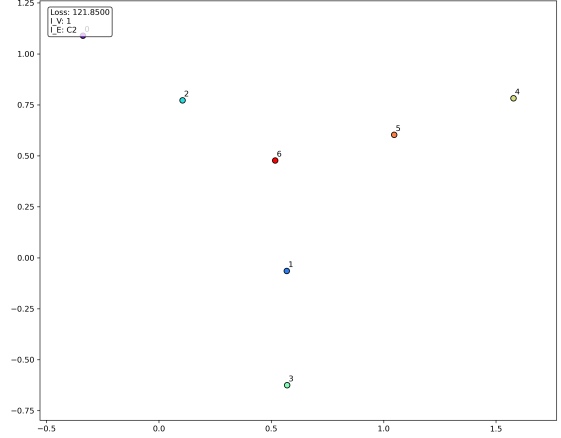


Figure 58

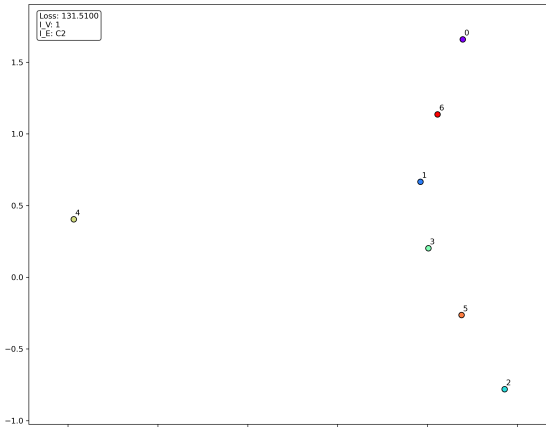


Figure 59

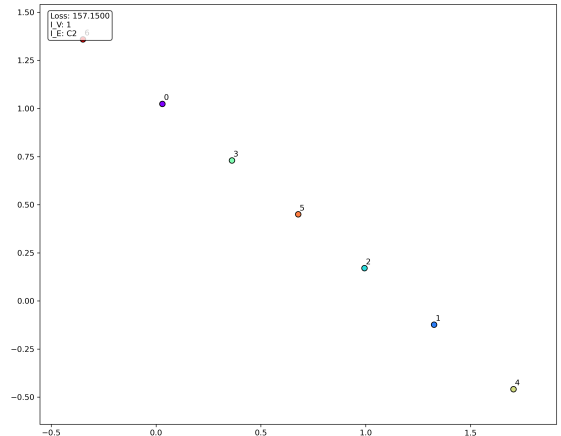


Figure 60

C Symmetry in Loss Landscapes: Particle Attraction vs. Random Polynomial Experiments

In this section, we present two complementary experiments. In the first experiment, we study a symmetric particle attraction loss function, and in the second, we examine a random homogeneous polynomial with similar bounded-below properties. The purpose is to compare the number of observable local minima in both settings and to discuss how symmetry may serve as a mechanism to limit the effective number of minima.

D Symmetric Particle Attraction Experiment

Consider points $x_1, \dots, x_4 \in \mathbb{R}^2$ and define the kernel

$$\kappa(x_i, x_j) = \langle x_i, x_j \rangle^8 - \langle x_i, x_j \rangle^3,$$

with the total energy (loss) function given by

$$L(x_1, \dots, x_4) = \sum_{i,j} \kappa(x_i, x_j).$$

Since the potential is invariant under any 2D isometry applied simultaneously to all particles (due to the inner product), the loss is invariant under the full orthogonal group O_2 . To eliminate the trivial isometry symmetry, we fix the second coordinate of the first particle to be zero. This choice reduces the ambient space from \mathbb{R}^8 (with four particles in \mathbb{R}^2) to \mathbb{R}^7 and provides a canonical representative under the O_2 action. In addition, a sign symmetry remains (multiplying all x - or all y -coordinates by -1), and the particle permutation symmetry group S_4 (restricted to those permutations that preserve the fixed second coordinate of the first particle) continues to act on the configuration.

Using 30×10^6 randomly generated initial points, Gradient Descent converged to only 4 distinct orbits of local minima. In other words, the system exhibits 4 types of local minima, and when the group actions are taken into account, there are a total of 54 observable local minima. The following is a summary of the minima types:

- **Type P_1 :** 2 minima with

$$P_1 = \begin{bmatrix} 0.906 & 0 \\ 0.906 & 0 \\ 0.906 & 0 \\ 0.906 & 0 \end{bmatrix}, \quad L(P_1) = -5.55.$$

- **Type P_2 :** 12 minima with

$$P_2 = \begin{bmatrix} 0.906 & 0 \\ 0.906 & 0 \\ 0 & 0.906 \\ 0 & 0.906 \end{bmatrix}, \quad L(P_2) = -2.77.$$

- **Type P_3 :** 16 minima with

$$P_3 = \begin{bmatrix} 0.906 & 0 \\ 0.906 & 0 \\ 0.906 & 0 \\ 0 & 0.906 \end{bmatrix}, \quad L(P_3) = -3.46.$$

- **Type P_4 :** 24 minima with

$$P_4 = \begin{bmatrix} 0.90146749 & 0 \\ 0.90146749 & 0 \\ -0.34181185 & -0.77588592 \\ -0.34181185 & 0.77588592 \end{bmatrix}, \quad L(P_4) = -1.51.$$

Thus, a total of 54 distinct local minima (accounting for all symmetry-related orbits) were observed in the symmetric case.

E Particle Attraction Case For Random 4 degree kernel

We conducted several experiments using different fourth-degree polynomial loss functions. Each experiment uses a different polynomial, detailed in the Appendix. The results are summarized in Table 11.

Table 11: Experimental Results

Experiment	Isotropy Group	Final Positions	Final Loss
1	Order: 8 Structure: D_4	$v_0 = 0.68269$	-9.009
		$v_1 = 0.28440$	
		$v_2 = 0.68269$	
		$v_3 = 0.68269$	
		$v_4 = 0.53480$	
2	Order: 6 Structure: S_3	$v_0 = -0.55875$	-14.536
		$v_1 = 0.93261$	
		$v_2 = 0.93261$	
		$v_3 = 0.93261$	
		$v_4 = -0.55875$	
3	Order: 48 Structure: $C_2 \times S_4$	$v_0 = -0.31517$	-5.7053
		$v_1 = -0.31517$	
		$v_2 = -0.31517$	
		$v_3 = -0.31517$	
		$v_4 = -0.31517$	
4	Order: 48 Structure: $C_2 \times S_4$	$v_0 = 0.29563$	-2.4287
		$v_1 = 0.29563$	
		$v_2 = 0.29563$	
		$v_3 = 0.29563$	
		$v_4 = 0.29563$	
5	Order: 6 Structure: S_3	$v_0 = 0.50970$	-2.1555
		$v_1 = 0.50970$	
		$v_2 = 0.50970$	
		$v_3 = -0.37541$	
		$v_4 = -0.37541$	
		$v_5 = -0.37541$	

Loss Functions for Each Experiment

In each experiment, the loss function L is a fourth-degree polynomial defined over the variables a_1, a_2, b_1, b_2 , corresponding to the edge vectors in the graph. The coefficients and monomials used in each experiment are listed below. We chose 30 monomials out of the 70 monomials of degree 4 in 4 variables. The coefficients were randomly chosen from a standard normal distribution. Where for the 4 degree coefficients is positive and the exponents of 4 degree monomials is even, I used this conditions to ensure the polynomial is bounded below.

Experiment 1:

$$\begin{aligned}
f(a, b) = & -0.3391 b_2 + 0.4791 a_1^4 + 0.1360 a_1 b_1^2 + 0.2717 a_2 b_1 b_2^2 - 0.5321 a_1 b_2 - 0.9043 b_1^2 \\
& + 0.7399 a_2 b_2 + 0.1840 b_2^3 + 0.6584 b_1 b_2 - 0.8382 a_1 b_2^2 + 0.8152 a_2^2 b_2 - 0.1054 a_1 \\
& + 0.5557 a_1^3 b_2 + 0.1230 a_1 a_2^2 b_1 - 0.7825 a_2^2 b_1 + 0.5794 a_1 a_2 b_1 b_2 - 0.8400 a_2^3 \\
& - 0.9640 b_2 + 0.8577 a_2 - 0.4882 b_1 + 0.4577 a_1^2 b_2 + 0.3470 b_2^2 + 0.4239 a_1^3 \\
& - 0.3558 a_2^2 + 0.4574 b_2^4 - 0.1283 b_1^2 b_2 + 0.9085 b_2 - 0.5772 a_1 a_2 - 0.8940 a_1^2 a_2 \\
& + 0.2102 a_2^2 b_1.
\end{aligned}$$

Experiment 2:

$$\begin{aligned}
f(a, b) = & 0.3677 a_1^2 a_2 b_1 - 0.0404 a_2 b_2^2 + 0.8227 a_1^4 + 0.7633 a_1 + 0.6529 a_2 + 0.0127 a_2^2 b_1 \\
& + 0.6695 a_2^3 b_1 + 0.7561 a_2 b_1^3 + 0.2934 a_1^3 b_1 - 0.8204 a_2 b_2^2 + 0.7910 a_2^2 b_2^2 \\
& + 0.5344 a_1 - 0.8581 a_2^2 + 0.5033 b_1^4 - 0.9312 a_1^3 + 0.5393 b_1 b_2^2 + 0.9664 a_2 b_1 b_2^2 \\
& + 0.1014 a_2 b_2 - 0.3991 b_2^3 - 0.8326 b_2 + 0.2821 a_1 b_2^2 + 0.0106 a_1 a_2 - 0.7970 a_1 \\
& + 0.8012 a_1 a_2^2 + 0.9380 a_1 a_2 b_1^2 - 0.2501 a_2^2 b_2 + 0.3412 b_2^3 + 0.9164 a_1 b_2 \\
& - 0.5956 a_2 + 0.2598 a_2^2 b_2.
\end{aligned}$$

Experiment 3:

$$\begin{aligned}
f(a, b) = & 0.9736 b_1^2 b_2 + 0.4452 a_1^2 a_2 b_2 + 0.6006 b_1^4 + 0.3478 a_2^2 b_1 b_2 - 0.0799 b_2 \\
& + 0.7705 b_1 b_2^3 - 0.0882 a_1 b_1 + 0.2263 a_1^2 b_1^2 + 0.0047 a_2 b_1 b_2 - 0.6979 a_2 b_2^2 \\
& + 0.8158 a_1 b_1^3 - 0.5612 a_1 b_2 - 0.7512 a_1 b_2^2 + 0.6146 a_2 b_1^2 b_2 + 0.9060 a_1^3 b_2 \\
& + 0.3293 a_1 b_1 b_2^2 - 0.4857 a_1 b_2 + 0.6202 a_1 + 0.7917 a_1^2 b_2^2 + 0.7527 b_1^2 b_2 \\
& + 0.4912 a_1 a_2^2 b_1 + 0.6479 a_1 a_2^2 b_2 - 0.0854 a_2^3 + 0.4726 a_2 b_1^3 - 0.1148 b_1 \\
& + 0.2498 b_2^4 + 0.2668 a_2^3 b_1 + 0.2609 a_1 a_2 b_1^2 + 0.3574 a_1 b_1^2 b_2 + 0.9839 a_1^2 a_2 b_1.
\end{aligned}$$

Experiment 4:

$$\begin{aligned}
f(a, b) = & 0.8046 a_2^3 b_1 - 0.0903 a_1 a_2 b_1 - 0.3022 a_2 b_1^2 + 0.7107 a_1 a_2 b_2^2 + 0.3738 a_1^2 a_2^2 \\
& + 0.4659 a_1 a_2 b_1 - 0.5364 a_2 b_1 b_2 + 0.4696 a_1 b_1^2 b_2 + 0.2321 a_1 b_2 + 0.4971 a_2^2 b_1 b_2 \\
& + 0.6020 a_1 a_2^3 - 0.8185 a_1 - 0.9552 a_1^2 b_1 - 0.9612 a_2^3 + 0.1544 a_2^2 b_1 + 0.9042 b_1^2 b_2^2 \\
& + 0.4775 b_2 + 0.4483 a_1 a_2 b_2 + 0.8384 a_1 b_2 - 0.8172 a_1 a_2^2 + 0.5101 b_1^3 \\
& + 0.3645 b_1 b_2^2 + 0.8480 a_1 b_1^3 + 0.2504 a_1 a_2^2 b_1 - 0.7310 a_1 b_2 + 0.4990 b_2^3 \\
& + 0.3686 a_2 b_1 b_2 - 0.6202 b_1^3 - 0.2180 a_2 b_2^2 + 0.0190 a_1.
\end{aligned}$$

Experiment 5:

$$\begin{aligned}
f(a, b) = & 0.6114 a_1 a_2^2 b_1 - 0.1573 a_1 a_2 - 0.4525 b_2^2 + 0.5590 b_1 b_2^3 + 0.5904 a_1 b_2 \\
& + 0.4621 a_2^2 + 0.9355 a_1^4 - 0.7042 a_1 a_2 b_2 - 0.5839 a_1^2 + 0.4718 a_1 b_1 \\
& + 0.1064 b_1^2 b_2^2 - 0.3174 a_1 b_1^2 - 0.3987 b_2 + 0.7050 a_1^3 a_2 + 0.5159 a_1 a_2 b_1 b_2 \\
& + 0.2817 a_2 b_2^3 + 0.3154 a_1^2 a_2^2 + 0.9684 b_1 - 0.3450 a_2 + 0.9796 a_1 b_1^2 \\
& + 0.9411 a_2^4 + 0.9193 a_1 b_1 b_2^2 + 0.6704 a_2^2 b_1 b_2 + 0.1101 a_1 b_1^3 \\
& + 0.1491 a_1 b_1 - 0.6584 a_1 + 0.9249 a_1 b_1 b_2 + 0.6863 a_1 b_1^2 b_2 + 0.3818 a_1 b_2^3 \\
& + 0.0884 a_2 b_2.
\end{aligned}$$

References

- Yossi Arjevani and Michael Field. On the principle of least symmetry breaking in shallow ReLU models. *arXiv preprint arXiv:1912.11939*, 2019. URL <https://arxiv.org/pdf/1912.11939>.
- Yossi Arjevani, Joan Bruna, Michael Field, Joe Kileel, Matthew Trager, and Francis Williams. Symmetry breaking in symmetric tensor decomposition. *arXiv preprint arXiv:2103.06234*, 2021. URL <https://arxiv.org/pdf/2103.06234>.